Convective outflow of South Asian pollution: A global CTM simulation compared with EOS MLS observations

Convective outflow of South Asian pollution: A global CTM simulation compared with EOS MLS observations

Qinbin Li,[1] Jonathan H. Jiang,[1] Dong L. Wu,[1] William G. Read,[1] Nathaniel J. Livesey,[1] Joe W. Waters,[1] Yongsheng Zhang,[2] Bin Wang,[3] Mark J. Filipiak,[4] Cory P. Davis,[4] Solene Turquety,[5] Shiliang Wu,[5] Rokjin J. Park,[5] Robert M. Yantosca,[5] and Daniel J. Jacob[5]

Received 22 February 2005; revised 13 May 2005; accepted 13 June 2005; published 28 July 2005.

[1] A global 3-D chemical transport model is used to analyze observations of carbon monoxide (CO) and upper tropospheric clouds from the EOS Microwave Limb Sounder (MLS). MLS observations during 25 August–6 September 2004 reveal elevated CO and dense high clouds in the upper troposphere over the Tibetan plateau and southwest China, collocating with the upper level Tibetan anticyclone. Model simulations indicate the transport of boundary layer pollution by Asian summer monsoon (ASM) convection and orographic lifting to the upper troposphere over South Asia, where simulated distributions of CO resemble MLS observations. Model results also show elevated aerosols in the anticyclone region. Analysis of model simulated CO and aerosols indicate that the Tibetan anticyclone could 'trap' anthropogenic emissions lifted from northeast India and southwest China. These aerosols may be responsible for the formation of some of the dense high clouds. **Citation:** Li, Q., et al. (2005), Convective outflow of South Asian pollution: A global CTM simulation compared with EOS MLS observations, *Geophys. Res. Lett.*, *32*, L14826, doi:10.1029/2005GL022762.

1. Introduction

[2] South Asia has been undergoing rapid industrial and economic development over the past two decades with increasing emissions of aerosols and gaseous pollutants. Quantifying the continental outflow and intercontinental transport of pollution from South Asia has been the focus of several recent studies [*Lelieveld et al.*, 2001]. In summer, South Asia is subjected to the influence of the Asian summer monsoon (ASM). Recent studies have suggested that deep convection associated with the ASM often lifts boundary layer (BL) pollution from India, Southeast Asia, and south China into the upper troposphere (UT) followed by westward transport by the tropical easterly jet to over the Middle East [*Li et al.*, 2001] and the Mediterranean [*Lelieveld et al.*, 2002]. Carbon monoxide (CO) plumes have been observed in the UT across South Asia in summer [*Kar et al.*, 2004]. The ASM circulation is also an important transport pathway for water vapor to the UT and lower stratosphere in the tropics [*Gettelman et al.*, 2004].

[3] The so-called Tibetan anticyclone (not always situated over Tibet) associated with the South Asia High (SAH) is one of the largest upper level anticyclones on Earth. *Li et al.* [2005] have pointed out that the upper level anticyclonic circulation over the southern United States in summer can trap convectively lifted pollution, leading to enhanced pollution in the UT over that region. It is conceivable that uplifted South Asia pollution could be 'trapped' by the Tibetan anticyclone. We show here that satellite observations of CO from the EOS Microwave Limb Sounder (MLS) [*Waters et al.*, 1999] and the Measurements of Pollution In The Troposphere (MOPITT) instrument [*Drummond*, 1992] support the aforementioned trapping effect. With a tropospheric lifetime of ~2 months CO is a sensitive tracer for transport of pollution [*Liu et al.*, 2003]. Simulations of CO and aerosols using the GEOS-CHEM global 3-D chemical transport model (CTM) [*Bey et al.*, 2001] are used to better understand the contributing processes. An important implication of this trapping effect is that the convectively lifted aerosols could potentially enhance high cloud formation.

2. Observations

[4] The EOS MLS was launched into orbit aboard the NASA Aura spacecraft on 15 July 2004. It has five radiometers measuring microwave emission of the Earth's atmosphere to retrieve chemical composition, temperature, and cloud ice. The retrievals are reported on fixed pressure levels [*Livesey*, 2004]. MLS chemical composition measurements in the UT are generally not degraded by the presence of clouds, since the typical particle sizes are much smaller than the wavelength of the radiation being observed. Here we use retrieved 147 hPa CO concentrations and cloud ice water content (IWC) for August 25–September 6, 2004, averaged on a 4° latitude by 8° longitude grid. Detailed descriptions of the retrieval of CO and clouds are presented by *Filipiak et al.* [2005] and *Wu and Jiang* [2004], respectively. At 147 hPa the CO and cloud IWC retrievals have respective precisions of ~25 ppb and ~1.8 mg/m^3, and both have a vertical resolution of ~4 km and a horizontal resolution of ~3° along the orbit. The MLS measurements

[1]Jet Propulsion Laboratory, California Institute of Technology, Pasadena, California, USA.
[2]International Pacific Research Center, School of Ocean and Earth Science and Technology, University of Hawai'i at Manoa, Honolulu, Hawaii, USA.
[3]Department of Meteorology and International Pacific Research Center, School of Ocean and Earth Science and Technology, University of Hawai'i at Manoa, Honolulu, Hawaii, USA.
[4]Institute of Atmospheric and Environmental Science, School of Geosciences, University of Edinburgh, Edinburgh, UK.
[5]Division of Engineering and Applied Sciences, Harvard University, Cambridge, Massachusetts, USA.

0094-8276/05/2005GL022762

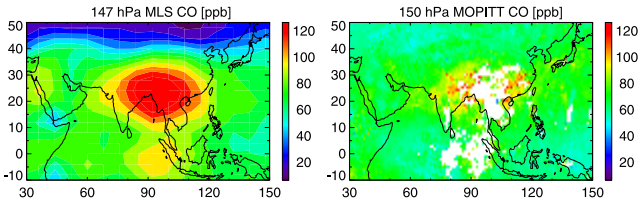

Figure 1. Concentrations of CO at 147 hPa from MLS and at 150 hPa from MOPITT. Values are averaged for the 10 MLS measurement days of 25–27, 29–31 August and 3–6 September 2004 (August 28 and September 1–2 are not retrieved because they either do not meet science team criteria or have not fit within MLS operational constraints). (right) White areas indicate missing data.

used here are MLS 1-D research product for CO (D. L. Wu, manuscript in preparation, 2005) and V1.4-CLD01 for cloud ice [*Wu and Jiang*, 2004].

[5] MOPITT is a nadir Infrared (IR) correlation radiometer launched aboard the NASA Terra spacecraft in 1999. It has solar backscatter channels to measure total CO columns, and IR emission channels to measure CO vertical profiles. The instrument provides global coverage from a polar orbit. Horizontal resolution is 22 km^2, and cross-track scanning achieves approximate global coverage in 3 days. CO concentrations are reported on 7 vertical levels, and as a total column, for cloud-free scenes. The MOPITT observations reported here are version 3 data with a 10% precision on both column and concentrations [*Deeter et al.*, 2003].

[6] MLS observed CO at 147 hPa shows a broad maximum (~130 ppb) over the Tibetan Plateau and south China (Figure 1). This maximum is also supported by MOPITT observations during the same time period, which show elevated CO concentrations (~120 ppb) at 150 hPa over the same region, but with missing data over much of southwest China due to cloud contamination (Figure 1). MLS can measure CO and cloud simultaneously [*Filipiak et al.*, 2005]. MLS observations show elevated cloud IWC collocated with the CO maximum during the same time period (Figure 2). These dense high clouds are accompanied with relatively little precipitation, as indicated by the CMAP [*Xie and Arkin*, 1996] precipitation rate, compared with the heavy precipitation associated with the deep convective clouds over the northern Indian Ocean (Figure 2). A large fraction of the high clouds have relatively small particle sizes (<30 μm), and are thus distinguished from convective clouds which have larger particles (D. L. Wu, manuscript in preparation, 2005). While large-scale condensation in the UT likely plays an important role in forming these high clouds, we propose that the uplifted BL aerosols trapped by the Tibetan anticyclone, as discussed in section 3, could enhance high cloud formation. The nature of the uplifted aerosols-high cloud interaction and the consequence on precipitation clearly needs further investigation and is beyond the scope of this study. The radiative forcing associated with high ice clouds generally acts to warm the Earth-atmosphere system, but the sign of the feedback (positive or negative) depends on both cloud IWC and ice crystal size [*Liou*, 2005].

3. Model Description and Simulations

[7] To examine the transport of South Asia pollution to the UT, we use GEOS-CHEM (v7.1.2) to conduct a simulation for August–September 2004. The model is driven by the GEOS-4 assimilated meteorological data from the NASA Global Modeling and Assimilation Office (GMAO), available every 6 hours with 1° × 1.25° horizontal resolution and 55 vertical layers. We average them over a 2° × 2.5° grid and lump the vertical grid into 30 layers. GEOS-CHEM simulation of tropospheric chemistry includes a detailed ozone-NOx-hydrocarbon chemical mechanism. Simulations of aerosols have been reported previously for black carbon (BC) and organic carbon (OC) [*Park et al.*, 2003] and sulfate aerosols [*Park et al.*, 2004]. Secondary organic aerosols are not included. Emissions and depositions are mostly described by *Bey et al.* [2001] and *Park et al.* [2003, 2004]. Anthropogenic emissions of BC and OC are from *Cooke et al.* [1999]. Biofuel and biomass burning emissions are from *Yevich and Logan* [2003] and *Duncan et al.* [2003], respectively.

[8] Figure 3 shows GEOS-CHEM simulated concentrations of CO and aerosols at 150 hPa, averaged for 25 August–6 September. Since the emissions in the model are not tailored for the MLS observation period, the focus of our comparison is on large-scale features rather than absolute concentrations. The winds during ASM are associated with a large scale cyclonic vorticity in the lower troposphere and the low level southwesterly jet over the Arabian Sea and the Tibetan anticyclone in the UT with its southern branch being the monsoon easterly jet, a well-known feature of the ASM circulation [*Krishnamurti and Bhalme*, 1976]. The Tibetan anticyclone is located over the eastern Tibetan Plateau during 25 August–6 September, associated with a well organized high pressure system centered around 95°E and 28°N, in both the GEOS-4 (Figure 3) and NCEP analyses, with the easterly jet south of 25°N. Elevated concentrations of CO and aerosols are

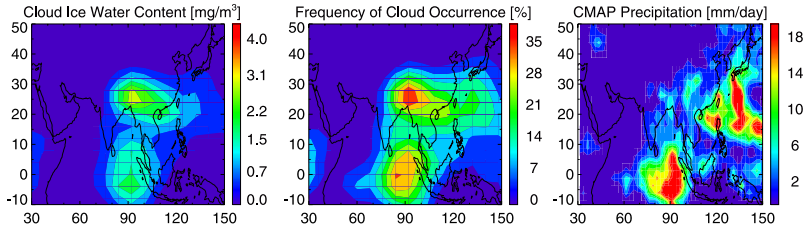

Figure 2. MLS retrieved 147 hPa cloud IWC (mg m^{-3}) and occurrence frequency (%) and CMAP precipitation rate (mm day^{-1}), averaged for the 10 days as in Figure 1.

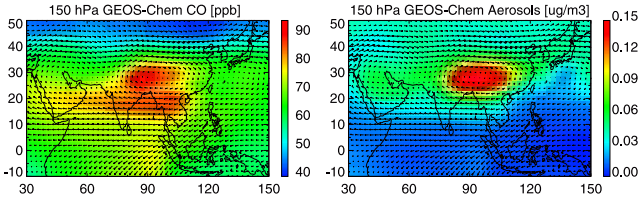

Figure 3. GEOS-CHEM simulated concentrations of CO and aerosols at 150 hPa, averaged for the 10 dates as in Figure 1. Also shown are GMAO horizontal winds.

seen collocated with the high pressure system. Enhanced CO is also seen over the Bay of Bengal, transported in the easterly jet. Such transport may not be distinguishable from circulation around the anticyclone in the MLS observations considering its horizontal resolution of 4° × 8°. Elevated aerosols are not seen in the UT over the Bay of Bengal due to efficient wet scavenging (Figure 2).

[9] Both CO and carbonaceous aerosols are products of incomplete combustion. Sulfur dioxide (SO_2) emissions are primarily from coal-fired power plants. Emissions of these pollutants in Asia are dominated by China and India (Figure 4). The industrial and residential sector, consisting of the combustion of coal and biofuels, generates the majority of the emissions of BC and OC, while emissions from natural sources are negligible [*Streets et al.*, 2003]. South of 35°N, emissions are concentrated in the Sichuan basin in southwest China and the Ganges plain in northeast India. Biomass burning emissions are relatively small at this time of the year except for Indonesia [*Duncan et al.*, 2003]. The broad distribution of BC and OC emissions reflects the prevalence of domestic coal and biofuel combustion across the rural areas.

[10] The prevailing winds in the BL are northwesterly over the Indian subcontinent, southwesterly over Southeast Asia, and northeasterly over south China (Figure 5). Note the low-level convergence in southwest China between the Indo-China southwesterly and the east China northeasterly. This low-level convergence plays an important role in lifting pollution upward as evidenced by the meridional cross section along 105°E (Figure 5) and the enhanced deep convective activity in southwest China. The southwesterly flow over Bangladesh and northern Southeast Asia encounters the southern slope of the Himalayas, results in orographic and convective lifting of pollution in northeast India and Bangladesh (Figure 5). During 24–26 August, typhoon Aere swept southeast China, and a broad low pressure associated with the remnant of Aere continued to affect the region through early September. The cyclonic circulation (northeasterly over east China) favors transport of pollution from the source regions toward the convergence zone around 20°N, where lifting into the UT takes place by frequent deep convection [*Liu et al.*, 2003]. Once in the UT, the pollution circulates southward and then westward in the easterly jet around the SAH, leading to enhanced CO concentrations over the Bay of Bengal in the model (Figure 3). A large fraction of this pollution is frequently entrained into and circulates around the anticyclonic circulation for several days. The enhanced concentrations of CO and aerosols around 5°S (Figure 5) reflect biomass burning in Indonesia (Figure 4).

[11] Model results thus indicate that the high concentrations of CO and aerosols at 20°N–40°N over the Tibetan plateau are primarily from convectively and orographically lifted anthropogenic emissions from northeast India and southwest China and entrained by the Tibetan anticyclone. By September 10, the anticyclone has moved westward to over the Persian Gulf, effectively ending the enhancements of pollution. It is not inconceivable that a combination of the slow-down of the easterly jet and the outflow over the Indian region could lead to the enhanced CO in the MLS observations. This however cannot explain the high CO north of 25°N (Figure 1). Clearly more observations are needed to further examine the impact of upper level circulation on convective South Asian pollution outflow.

4. Summary and Discussions

[12] EOS MLS observations during 25 August–6 September 2004 reveal elevated CO concentrations in the UT over the Tibetan plateau, accompanied by dense high clouds and little precipitation as indicated by CMAP precipitation rate. Simulations of CO and aerosols with the GEOS-CHEM global 3-D CTM driven by assimilated meteorological data indicate that anthropogenic emissions from northeast India and southwest China are transported into the UT and part of the pollution is entrained by the upper level Tibetan anticyclone. Comparative analyses of MLS upper tropospheric observations and the model simulations provide some evidence for this 'trapping'.

[13] The dense high clouds in the UT over the Tibetan plateau may be related to the convectively and orographically lifted anthropogenic aerosols from South Asia. Cloud formation and its microphysical properties are strongly influenced by the availability of aerosols. An increase in

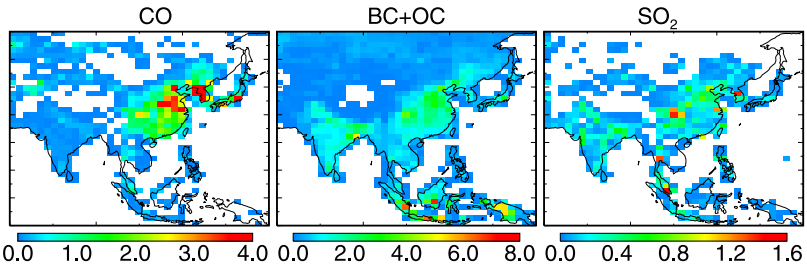

Figure 4. Emissions of CO, BC+OC, and SO_2 in Asia in 25 August–6 September from anthropogenic and biomass burning.

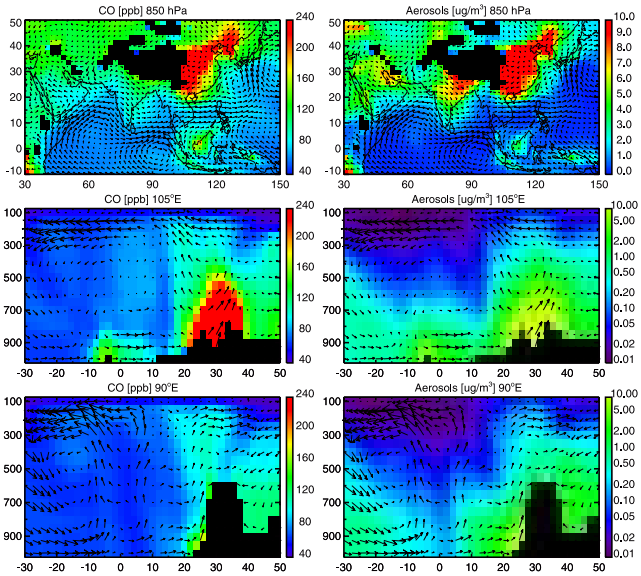

Figure 5. GEOS-CHEM simulated concentrations of CO and aerosols at 850 hPa and along 105°E and 90°E, averaged for the 10 dates as in Figure 1. Aerosol concentrations along 105°E and 90°E are plotted on logarithmic scale. The constant CO concentrations above 150 hPa indicate model stratosphere. Also shown are NCEP winds with vertical velocity multiplied by a factor of 1000. Dark areas indicate topography.

aerosols from anthropogenic emissions transported to the UT could conceivably lead to more high clouds with small particle size. Changes in cloud properties could have profound impact on the global cloud system, hydrological cycle, and climate.

[14] **Acknowledgments.** This work was performed at Jet Propulsion Laboratory, California Institute of Technology, under contract with NASA. We thank all colleagues and associates for contributing to the MLS project. We also thank Jean-Pierre Blanchet for helpful comments. The GEOS-CHEM model is managed at Harvard University with support from the NASA ACMAP program. We also acknowledge the support by UK Natural Environment Research Council and University of Hawaii.

References

Bey, I., D. J. Jacob, R. M. Yantosca, J. A. Logan, B. D. Field, A. M. Fiore, Q. Li, H. Y. Liu, L. J. Mickley, and M. G. Schultz (2001), Global modeling of tropospheric chemistry with assimilated meteorology: Model description and evaluation, *J. Geophys. Res.*, *106*, 23,073–23,089.

Cooke, W. F., C. Liousse, H. Cachier, and J. Feichter (1999), Construction of a 1° × 1° fossil fuel emission data set for carbonaceous aerosol and implementation and radiative impact in the ECHAM-4 model, *J. Geophys. Res.*, *104*, 22,137–22,162.

Deeter, M. N., et al. (2003), Operational carbon monoxide retrieval algorithm and selected results for the MOPITT instrument, *J. Geophys. Res.*, *108*(D14), 4399, doi:10.1029/2002JD003186.

Drummond, J. R. (1992), Measurements of Pollution in the Troposphere (MOPITT), in *The Use of EOS for Studies of Atmospheric Physics*, pp. 1269–1284, Elsevier, New York.

Duncan, B. N., R. V. Martin, A. C. Staudt, R. Yevich, and J. A. Logan (2003), Interannual and seasonal variability of biomass burning emissions constrained by satellite observations, *J. Geophys. Res.*, *108*(D2), 4100, doi:10.1029/2002JD002378.

Filipiak, M. J., R. S. Harwood, J. H. Jiang, Q. Li, N. J. Livesey, G. L. Manney, W. G. Read, M. J. Schwartz, J. W. Waters, and D. L. Wu (2005), Carbon monoxide measured by the EOS Microwave Limb Sounder on Aura: First results, *Geophys. Res. Lett.*, *32*, L14825, doi:10.1029/2005GL022765.

Gettelman, A., D. E. Kinnison, T. J. Dunkerton, and G. P. Brasseur (2004), Impact of monsoon circulations on the upper troposphere and lower stratosphere, *J. Geophys. Res.*, *109*, D22101, doi:10.1029/2004JD004878.

Kar, J., et al. (2004), Evidence of vertical transport of carbon monoxide from Measurements of Pollution in the Troposphere (MOPITT), *Geophys. Res. Lett.*, *31*, L23105, doi:10.1029/2004GL021128.

Krishnamurti, T. N., and H. N. Bhalme (1976), Oscillations of a monsoon system, part I: Observational aspect, *J. Atmos. Sci.*, *33*, 1937–1953.

Lelieveld, J., et al. (2001), The Indian Ocean Experiment: Widespread air pollution from south and Southeast Asia, *Science*, *291*, 1031–1036.

Lelieveld, J., et al. (2002), Global air pollution crossroads over the Mediterranean, *Science*, *298*, 794–799.

Li, Q. B., et al. (2001), A tropospheric ozone maximum over the Middle East, *Geophys. Res. Lett.*, *28*, 3235–3238.

Li, Q., D. J. Jacob, R. Park, Y. Wang, C. L. Heald, R. Hudman, R. M. Yantosca, R. V. Martin, and M. Evans (2005), North American pollution outflow and the trapping of convectively lifted pollution by upper-level anticyclone, *J. Geophys. Res.*, *110*, D10301, doi:10.1029/2004JD005039.

Liou, K. N. (2005), Cirrus clouds and climate, in *McGraw-Hill 2005 Yearbook of Science and Technology*, New York.

Liu, H., D. J. Jacob, I. Bey, R. M. Yantosca, B. N. Duncan, and G. W. Sachse (2003), Transport pathways for Asian pollution outflow over the Pacific: Interannual and seasonal variations, *J. Geophys. Res.*, *108*(D20), 8786, doi:10.1029/2002JD003102.

Livesey, N. J. (2004), EOS MLS retrieval processes algorithm theoretical basis, *Jet Propul. Lab. Doc. D-16159*, Pasadena, Calif.

Park, R. J., D. J. Jacob, M. Chin, and R. V. Martin (2003), Sources of carbonaceous aerosols over the United States and implications for natural visibility, *J. Geophys. Res.*, *108*(D12), 4355, doi:10.1029/2002JD003190.

Park, R. J., D. J. Jacob, B. D. Field, R. M. Yantosca, and M. Chin (2004), Natural and transboundary pollution influences on sulfate-nitrate-ammonium aerosols in the United States: Implications for policy, *J. Geophys. Res.*, *109*, D15204, doi:10.1029/2003JD004473.

Streets, D. G., et al. (2003), An inventory of gaseous and primary aerosol emissions in Asia in the year 2000, *J. Geophys. Res.*, *108*(D21), 8809, doi:10.1029/2002JD003093.

Waters, J. W., et al. (1999), The UARS and EOS Microwave Limb Sounder Experiments, *J. Atmos. Sci.*, *56*, 194–218.

Wu, D. L., and J. H. Jiang (2004), EOS MLS algorithm theoretical basis for cloud measurements, *Jet Propul. Lab. Doc. D-19299*, Pasadena, Calif.

Xie, P., and P. A. Arkin (1996), Analyses of global monthly precipitation using gauge observations, satellite estimates, and numerical model predictions, *J. Clim.*, *9*, 840–858.

Yevich, R., and J. A. Logan (2003), An assessment of biofuel use and burning of agricultural waste in the developing world, *Global Biogeochem. Cycles*, *17*(4), 1095, doi:10.1029/2002GB001952.

C. P. Davis and M. J. Filipiak, Institute of Atmospheric and Environmental Science, School of Geosciences, University of Edinburgh, James Clerk Maxwell Building, The King's Buildings, Mayfield Road, Edinburgh EH9 3JZ, UK.

D. J. Jacob, R. J. Park, S. Turquety, S. Wu, and R. M. Yantosca, Division of Engineering and Applied Sciences, 29 Oxford Street, Harvard University, Cambridge, MA 02138, USA.

J. H. Jiang, Q. Li, N. J. Livesey, W. G. Read, J. W. Waters, and D. L. Wu, Jet Propulsion Laboratory, California Institute of Technology, 4800 Oak Grove Drive, M/S 183-501, Pasadena, CA 91109, USA. (qinbin.li@jpl.nasa.gov)

B. Wang, Department of Meteorology and International Pacific Research Center, School of Ocean and Earth Science and Technology, University of Hawai'i at Manoa, 1680 East West Road, Post Bldg. 401, Honolulu, HI 96822–2219, USA.

Y. Zhang, International Pacific Research Center, School of Ocean and Earth Science and Technology, University of Hawai'i at Manoa, 2525 Correa Road, Honolulu, HI 96822–2219, USA.